International Journal of Control, Automation and Systems VV(X) (YYYY) 1-3
http://dx.doi.org/10.1007/s12555-xxx-xxxx-xx
ISSN:1598-6446 eISSN:2005-4092
http://www.springer.com/12555

Robust control for electric fuel pump with variant nonlinear loads based on a new combined sliding mode surface

Runze Ding, Lingfei Xiao*

Abstract: A class of electric fuel pump system equipped in More-electric Engines with variant loads is studied. A novel robust control method based on a combined linear and quadratic integral sliding mode surface is proposed. The linear sliding mode surface with improved exponential reaching law guarantees that nominal system has satisfying performance with reduced chattering, while the quadratic integral sliding mode surface is responsible for compensation of mismatched uncertainties, enhancing system's robustness. Besides, mathematical model of electric fuel pump with variant load and leakages is established, which reflects both steady and dynamic characteristics of the fuel pump. In addition, it is proved that combined sliding mode surface can be reached in finite time and remains there. Stability of closed-loop system is proved as well. The effectiveness of the proposed method is verified by simulation results.

Keywords: Electric fuel pump, Combined sliding mode surface, Mismatched uncertainties, Robust control

1. INTRODUCTION

MEE(More-electric Engine), an innovative architecture for aircraft engines seeking for efficiency improvements in engine system(Fig.1),have gained much attention in recent decades, mainly for their predicted fuel economy and reduced carbon emissions[1-3] .

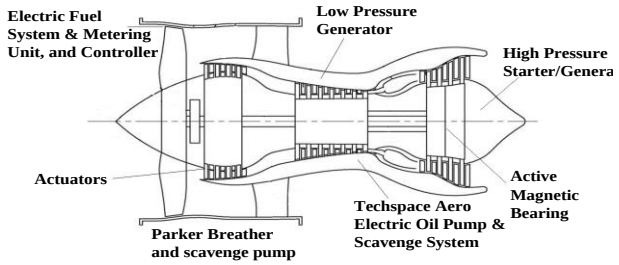

Fig.1 Structure of More-electric Engine

The major concept of MEE is changing power source for accessories from mechanical/hydraulic to the electric power, in other words, conventional AGB (Accessory Gear Box)-driven pumps and hydraulic actuators are replaced with electric motor-driven pumps and EMAs(Electro-Mechanical Actuators) driven by generators. Consequently, a major task of MEE is developing the electric fuel system, which is the key of More Electric Architechture[4] , integrating propulsion system (MEE) and the MEA(More Electric Aircraft) system.

EFP(electric motor-driven fuel pump, shown in Fig.2), the core component of electric fuel system, is composed of a gear pump and a motor, which is mainly a BLDC(brushless direct current motor), with intelligent controllers. Its applications will have great impacts on traditional fuel system(In Fig.2, A/C stands for Alternating Current and Wf stands for Fuel Flow).

Conventional fuel system for aircraft engines is based on AGB-driven pump, which is generally a fixed displacement pump. The speed of pump is proportionally related to engine speed. As a result, the pump will provide much greater flow than actual need, resulting in bypassing excess fuel flow. The flow of excess fuel can be several times greater than real need, leading to inefficiencies and other unsatisfying outcomes[5].

As a contrary, the fuel flow of electric fuel system can be controlled according to FADEC[6,7](Full Authority Digital Engine Control) demands(Fig.3), eliminating flowing back. Besides, the electric motor-driven fuel

This journal was supported by the Fundamental Research Funds for the Central Universities (NS2016027) and the Nanjing University of Aeronautics and Astronautics Graduate Innovation Base (Laboratory) Open Fund (kfjj20170211, kfjj20170219)

Runze Ding, Lingfei Xiao are with College of Energy and Power Engineering, Jiangsu Province Key Laboratory of Aerospace Power Systems, Nanjing University of Aeronautics and Astronautics, 29 Yudao Street, 210016, Nanjing, China.(e-mail: lfxiao@nuaa.edu.cn)
* Corresponding author.

ICROS, KIEE and Springer 2016

pump system also improves engine oil heat management, and allows ACOC(Air-Cooled Oil Cooler) to be eliminated[8], avoiding a series of issues including increased temperature of fuel and power loss caused by wasting fan discharge air. Moreover, the fuel bypass is removed and AGB is simplified to enhance engine efficiency with improved SFC(Specific Fuel Consumption)[9]. Therefore, the electric fuel system will contribute to the reduction of engine power extraction to drive the fuel pump, leading to an improvement in engine efficiency. In addition, the engine system reliability will be improved.

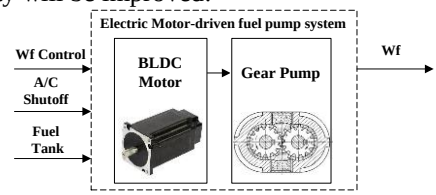

Fig.2 Structure of Electric Motor-driven Fuel Pump System

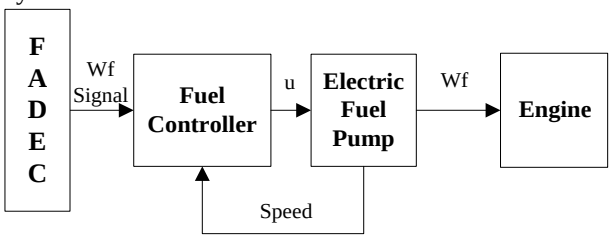

Fig.3 Control Structure of Electric Fuel System

However, there are challengesr in applying new electric fuel system in MEE and one of key technical barrier is robust controller design. After the application of EFP, the pump discharges exact fuel flow demanded by the FADEC, resulting in that a large part of performance of engine is depended on the property of intelligent controllers, which is crucial for aircraft safety. Besides, the FMU(Fuel Management Unit)[9] is eliminated in MEE, leading to the situation that the EFP itself will be used as a metering device, setting new request for controllers including accuracy,good dynamic performance, reliability and robustness.

Many manufactures and researchers are starving to find solutions to improve controllers, and a series of attempts are made. Some progresses are achieved in fuel system modeling[10,11], energy management[12], as well as researches on electric fuel pump control applied in internal-combustion or vehicles[13-15]. But the research on these fields developed slowly. One reason is that many researches are based on hardware redundancy, with less works on control strategy. Another one is that some results are not suitable in aviation area. MEE is a class of nonlinear and tightly coupled system working under tough situations including high temperature and high speed for long-term. Tough environment makes parameters perturbations and external disturbances unavoidable. Moreover, the largest concern that affects pump accuracy is variations in pump performance, which are caused by manufacturing error of the pump part, declining volumetric efficiency, changes resulted by fuel temperature. Those factors bring system uncertainties. The challenges above-mentioned lead to a pressing need to an accurate controller with robustness to system uncertainties and external disturbances.

SMC(Sliding Mode Control) [16-18] is a classical variable structure robust control method. By choosing the sliding mode surface and the reaching law, SMC theoretically ensure perfect tracking performance with insensibility to external interferences and parameters variations. Its fruitful results in nonlinear dynamical system and uncertain system contributes to being a major branch in robust control. Wide applications can be found in areas concerned with robustness including spacecraft, aircraft engines, BLDC motors, fuel pump [19-24].

Nevertheless, the robustness of SMC is only achieved when system is in sliding mode, and its insensitivity is limited to uncertainties that satisfy matching condition[25,26]. In other words, SMC is vulnerable to mismatched uncertainties (uncertainties that do not satisfy matching condition) and robustness is not guaranteed when system is in reaching phase. To solve those problems, a series of methods are proposed [27-33] in uncertain system, like FISMC(Fuzzy Integral Sliding Mode Control), control based on integral fuzzy switching manifold. Among those attempts, an improved ISMC [34] with projection matrix is designed to enable uncertain system to be robust to mismatched uncertainties and eliminating reaching phase. Unfortunately, its result is proved to be conservative.

As an improvement, an innovative robust control method based on CSMC (Combined Sliding Mode Control) is proposed in this paper. CSMC expands SMC with an auxiliary control, to enhance the robustness to mismatched uncertainties and reduce the chattering. The SMC control u_0 deduced from linear sliding mode surface s_l is responsible for nominal system's(system without uncertainties) performance with reduced chattering. And an auxiliary control u_1 deduced from quadratic integral sliding mode surface s_q is focused on compensations to mismatched uncertainties, improving robustness. Improved exponential reaching law $\dot{s}_l$ ensures that the reaching speed is adaptive to system state and chattering is reduced. Via the act of u_0+u_1, CSMC will not only have the advantages of SMC including simple structure and insensitivity to matched uncertainties, but also be robust to mismatched uncertainties. Besides, CSMC guarantees that the system is on the sliding mode surface from any initial time, with stronger robustness to uncertainties, reducing conservativeness of controller. It is proved that CSMC is suitable for EFP system, which is a typical system with matched and mismatched uncertainties.

The primary contributions of this paper are as follows:

(1) Considering external disturbances and parameters perturbations, mathematical model of EFP system is established with detailed analysis on leakages.

(2) A novel robust control method (CSMC) is proposed based on combined sliding mode surface, to compensate both matched and mismatched uncertainties, achieving satisfying performance. CSMC is less conservative when compared to present results[34].

(3) Improved exponential reaching law guarantees an adaptive approaching speed according to system state. Adaptive approaching speed results rapid convergence

with reduced chattering.

(4) The theoretical proof of the reachability of combined sliding mode surface and the stability of closed-loop system is given based on Lyapunov theory.

(5) Detailed analysis of system in sliding mode is shown to theoretically prove CSMC's robustness to mismached uncertainties.

(6) Simulation is carried out in comparison with SMC to verify the effectiveness of CSMC.

The remainder of this paper is organized as following: The mathematical description of EFP and pump leakage are shown in Section 2. In Section 3, the structure of CSMC is introduced and analysis of system in sliding mode is given. The proof of reachability of CSMC and stability of closed-loop system are shown in Section 4. Section 5 gives the simulation results verifying the effectiveness of CSMC, and conclusions of this work are given in Section 6.

2. SYSTEM CONFIGURATION

The electric motor-driven fuel pump is composed of a BLDC motor system and an external gear pump. The motor is directly connected with the external gear pump, and the external gear pump is driven by the motor to discharge fuel.

External gear pump[35] is a class of widely used quantitative pump. External gear pump mainly consists of gear pump shell and external gears. The gear, which is directly connected to the driving motor, is called the driving wheel. And the other one is called the driven wheel. The instantaneous volume is changing when the gear is meshing and separating, realizing absorption from fuel tank and discharge of fuel to engine. The external gear pump has advantages of small size, light weight, simple structure, reliable work and good self-priming performance, leading to its wide applications in the fields of aerospace, agriculture, mechanical and hydraulic.

Mathematical descriptions of electric fuel pump are generally in form of transfer function or functions approximated by polynomials based on local linearization around a nominal operating point, with advantages of easy implementation, simple structure. Above-mentioned methods are based on real experimental data and strict assumption of small range operation to ensure the linear model to be valid. Nevertheless, the speed of gears are required to be adjustable in a wide range, in other words, the model need to be valid in a wide speed range. But system's responses change due to various factors like different pressure and speed, which will result that the models established in those ways are limited. Besides, the unavoidable leakages in gear pumps change under different working conditions, making models different. Consequently, a mathematical model based on dynamic analysis with detailed illustration of leakage is introduced in this section, paving ways for application of advanced control algorithms.

Assumptions in mathematical model are introduced as follows: 1. The transmission efficiency of gear drive is almost 0.95~0.99, thus the influence of transmission efficiency is omitted in kinetic analysis of the system. 2. The influence of eddy current loss is omitted and the magnetic field is uniform. The phase shift of BLDC motor is 120 electrical degree. 3. Drive circuit of BLDC motor is reasonably designed and the commutation ripples could be omitted. Detailed modeling procedures is shown in followings.

The motion of electric fuel pump could be described by following equations [36, 37]:

$$\begin{cases} \dfrac{d\theta_1}{dt}=\omega_1 \\ (J_1+J_3)\dfrac{d\omega_1}{dt}=2K_e i_a-R_e k_1(\omega_1-\omega_2)-R_e k_2(\theta_1-\theta_2)-M_1 \\ \dfrac{d\theta_2}{dt}=\omega_2 \\ J_2\dfrac{d\omega_2}{dt}=R_e k_1(\omega_1-\omega_2)+R_e k_2(\theta_1-\theta_2)-M_2 \\ \dfrac{di_a}{dt}=\dfrac{-R}{L}i_a-\dfrac{K_e}{L}+\dfrac{1}{2L}(u_a-u_b) \end{cases} \tag{1}$$

where θ_1 is angular displacement of the driving gear, θ_2 is angular displacement of the driven gear, ω_1 is angular velocity of the driving gear, ω_2 is angular velocity of the driven gear, J_1 is moment of inertia of the driving gear, J_2 is moment of inertia of the driven gear, R_e is radius of addendum, R_1 is circle radius of driving gear, R_2 is circle radius of driven gear, B is tooth thickness, Δp is pressure difference, $M_1 = \frac{1}{2}B\Delta p\left(R_e^2-R_1^2\right)$ is equivalent torque on driving gear, $M_2=\frac{1}{2}B\Delta p\left(R_e^2-R_1^2\right)$ is equivalent torque on driven gear, k_1 is equivalent damping coefficient, k_2 is equivalent stiffness coefficient, K_e is Back-EMF coefficient, i_a is current in BLDC motor in one phase, u_a、u_b are stator voltages, L is equivalent common reactance

The instantaneous flow of gear pump q_v could be illustrated as follows [38]:

$$q_v=\frac{1}{2}\omega_1 B\left[2R_1(h_1+h_2)+h_1^2+h_2^2\frac{R_1}{R_2}-\left(1+\frac{R_1}{R_2}\right)f^2\right] \tag{2}$$

where h_1 is addendum height of the driving gear, h_2 is addendum height of the driven gear, f is the distance between the engaging point and the pitch point. The gears studied in this paper is a pair of involute gear containing the same number of teeth, leading to $R_1=R_2=R$, $h_1=h_2=h$.

Based on geometric structure of gears, $h=R_e-R_1$ holds. Consequently, the instantaneous flow of gear pump will be:

$$q_v=\omega_1 B\left(R_e^2-R^2-f^2\right) \tag{3}$$

When the gear pump is not equipped with unloading groove[39], the theoretical flow of gear pump will be:

$$Q_v=\omega_1 B\left(R_e^2-R^2-\frac{kt_0^2}{12}\right) \tag{4}$$

where $k=4-6\varepsilon+3\varepsilon^2$, $\varepsilon=\frac{f_0}{t_0}$, and t_0 is the base pitch of gear, f_0 is the length of actual meshing line

Then Q_v could be written into:

$$Q_v=K_Q\omega$$

where $K_Q=B\left(R_e{}^2-R^2-\frac{kt_0{}^2}{12}\right)$

The internal leakage is inevitable in application of gear pump due to its physical structure, which unfortunately, will leave unsatisfying impact on performance of gear pump. Thus, the influence of internal leakage should be taken into consideration. The internal leakage is divided into two part, one is radial leakage and the other one is seal face leakage[39, 40].

The seal face leakage Q_l is commonly described as[40]:

$$Q_l=B\left(\frac{\Delta p}{6\mu Sz_0}h^3-2\pi\omega_1 h\right) \tag{5}$$

where μ is coefficient of kinetic viscosity of the working medium, z_0 is tooth number in transition zone and S is the tooth thickness on the addendum circle.

The radial leakage Q_s is introduced in the following equation[40]:

$$Q_s=\frac{2\pi h^3\Delta p}{6\mu\ln\left(\frac{R_f}{R_z}\right)} \tag{6}$$

where R_f is radius of dedendum circle, R_z is radius of gear shafts

As a result, the real flow of gear pump will be: $Q_r=Q_v-Q_l-Q_s$

To conclude, choosing state vector as $x_{\text{EFP}}=\left[x_1\ \ x_2\ \ x_3\ \ x_4\ \ x_5\right]^T=\left[\theta_1\ \ \theta_2\ \ \omega_1\ \ \omega_2\ \ i_a\right]^T$, the mathematical model of EFP will be:

$$\begin{cases}\dot{x}_{\text{EFP}}=f\left(x_{\text{EFP}}\right)+g\left(x_{\text{EFP}}\right)u+M\\ y=Cx_{\text{EFP}}+D\end{cases} \tag{7}$$

where

$$f(x_{\text{EFP}})=\begin{bmatrix}0 & 0 & 1 & 0 & 0\\ 0 & 0 & 0 & 1 & 0\\ \frac{-R_ek_2}{\left(J_1+J_3\right)} & \frac{R_ek_2}{\left(J_1+J_3\right)} & \frac{-R_ek_1}{\left(J_1+J_3\right)} & \frac{R_ek_1}{\left(J_1+J_3\right)} & \frac{2K_e}{\left(J_1+J_3\right)}\\ \frac{R_ek_2}{J_2} & \frac{-R_ek_2}{J_2} & \frac{R_ek_1}{J_2} & \frac{-R_ek_2}{J_2} & 0\\ 0 & 0 & \frac{-K_e}{L} & 0 & \frac{-R}{L}\end{bmatrix}\begin{bmatrix}x_1\\ x_2\\ x_3\\ x_4\\ x_5\end{bmatrix},$$

$g\left(x_{\text{EFP}}\right)=\left[0\ \ 0\ \ 0\ \ 0\ \ \frac{1}{2L}\right]^T$, M are unknown parameters perturbations and external disturbances, $u=u_a-u_b$ is the value of control voltage, D is disturbance in output and $D=\frac{B\Delta p}{6\mu Sz_0}h^3+\frac{2\pi h^3\Delta p}{6\mu\ln\left(\frac{R_f}{R_z}\right)}$, C is the gain matrix of output, $C=\left[0\ \ 0\ \ K\ \ 0\ \ 0\right]$, where $K=K_Q-2\pi Bh$.

Remark 1: Parameters perturbations and external disturbances M are uncertainties in system, which are generally unknown. However, it is acceptable to assume that M is norm-bounded. And the effects of M are equivalent to effects caused by unknown uncertainties in system state $\Delta f\left(x_{\text{EFP}}\right)$ and unknown uncertainties in control channel $\Delta g\left(x_{\text{EFP}}\right)$ .Consequently, the system could be written into

$$\begin{cases}\dot{x}_{\text{EFP}}=f\left(x_{\text{EFP}}\right)+\Delta f\left(x_{\text{EFP}}\right)+g\left(x_{\text{EFP}}\right)u+\Delta g\left(x_{\text{EFP}}\right)u\\ y=Cx_{\text{EFP}}+D\end{cases} \tag{8}$$

Remark 2: System (8) is a class of uncertain system with disturbances and uncertainties $\Delta f\left(x_{\text{EFP}}\right)$ and $\Delta g\left(x_{\text{EFP}}\right)$. There are output disturbances as well.

In the remainder of this paper, a control system with robustness to matched and mismatched uncertainties will be designed.

3. DESIGN OF COMBINED SLIDING MODE CONTROL

3.1. Controller structure

Consider an arbitrary uncertain system with matched and mismatched uncertainties as follow:

$$\dot{x}(t)=f(x)+\Delta f(x)+\left[g(x)+\Delta g(x)\right]u \tag{9}$$

where $x(t)\in R^n$ is the state vector, $u\in R$ is the control signal, $f(x)=\left[f_1(x)\ \ f_2(x)\ \ \ldots\ \ f_4(x)\right]^T$ is smooth nonlinear function of x, $g(x)=\left[g_1(x)\ \ g_2(x)\ \ \ldots\ \ g_4(x)\right]^T$ are nonlinear control gain vectors, $\Delta f(x)=\left[\Delta f_1(x)\ \ \Delta f_2(x)\ \ \ldots\ \ \Delta f_4(x)\right]^T$ and $\Delta g(x)u=\left[\Delta g_1(x)\ \ \Delta g_2(x)\ \ \ldots\ \ \Delta g_4(x)\right]^T u$ are parameters perturbations and external disturbances.

The nominal system (the system without uncertainties) is shown in (10)

$$\dot{x}=f(x)+g(x)u \tag{10}$$

Combined sliding mode surface consists of two sliding mode surface. One is a typical linear sliding mode surface s_l, and the other one s_q is an integral sliding mode surface in a quadratic form.

The combined sliding mode control law u will be designed as:

$$u=u_0+u_1 \tag{11}$$

The structure of CSMC is shown in Fig.2.

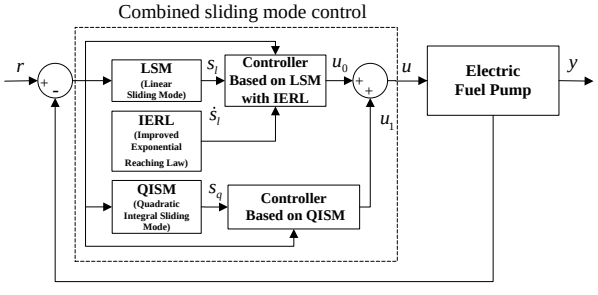

Fig.2 Structure of combined sliding mode control system

$u = u_0 + u_1$ is the total control act on system. The u_0 stands for SMC control action based on s_l, which is responsible for the performance of the nominal system and guarantees the robustness to matched uncertainties. u_1 stands for auxiliary control action based on quadratic integral sliding mode surface s_q, compensating the effects caused by mismatched uncertainties.

3.2. Analysis of linear sliding mode

The linear sliding mode surface s_l with an improved exponential reaching law $\dot{s}_l$ is defined as:

$$\begin{cases} s_l = C_l x(t) \\ \dot{s}_l = -\kappa_1 s_l - \dfrac{\kappa_2 |s_l|^{\alpha}}{N(s_l)} \operatorname{sgn}(s_l) \\ N(s_l) = \delta_0 + (1-\delta_0) e^{-\gamma |s_l|^{P}} \end{cases} \tag{12}$$

where $C_l \in R^{1\times n}$ is a gain matrix, $\dot{s}_l$ is the reaching law of s_l, $\kappa_1, \kappa_2 \in R$ are positive approaching parameters, α, δ_0, γ are strictly positive scalars and $0 < \alpha, \delta_0 < 1$, P is a strictly positive integer, $|\cdot|$ denotes the absolute value.

SMC control based on reaching law is designed to be:

$$u_0 = \left[C_l g(x)\right]^{-1} \left[-C_l f(x) + \dot{s}_l\right]$$

Remark 3: $N(s_l)$ is designed to be always strictly positive, guaranteeing the stability of system. When $|s_l|$ grows larger, $N(s_l)$ decrease and $\dfrac{\kappa_2 |s_l|^{\alpha}}{N(s_l)}$ become larger, accelerating approaching. When $|s_l|$ reaches 0, the chattering is reduced due to existence of the exponential term and the increase of $N(s_l)$.

Remark 4: It is apparently that $s_l \dot{s}_l < 0$, guaranteeing the reachability of s_l. When system is on s_l, the equivalent control[42] deduced from $\dot{s}_l = 0$ is $u_{0\text{eq}} = -\left[C_l g(x)\right]^{-1} C_l f(x)$. Substitute $u_{0\text{eq}}$ into (10), The closed-loop system will be $\dot{x} = \left[I - \left[C_l g(x,t)\right]^{-1} C_l\right] f(x)$. By choosing proper C_l, the poles of closed-loop system can be assigned to guarantee the stability of nominal system under u_0 control.

Advantages of $\dot{s}_l$ (slaw_3)will be shown in comparison with present results in exponetial reaching law[44,45](slaw_1 , slaw_2). Setting initial value of switching function to be $s_l(0) = 100$, simulation is carried out to explain the differences.

(1) $\text{slaw}_1 = -1 \times |s_l|^{0.5} \operatorname{sgn}(s_l)$

(2) $\text{slaw}_2 = -1 \times \left[0.1 + (1-0.1) e^{-|s_l|^2}\right]^{-1} \operatorname{sgn}(s_l)$

(3) $\text{slaw}_3 = -1 \times \left[0.1 + (1-0.1) e^{-|s_l|^2}\right]^{-1} |s_l|^{0.1} \operatorname{sgn}(s_l)$.

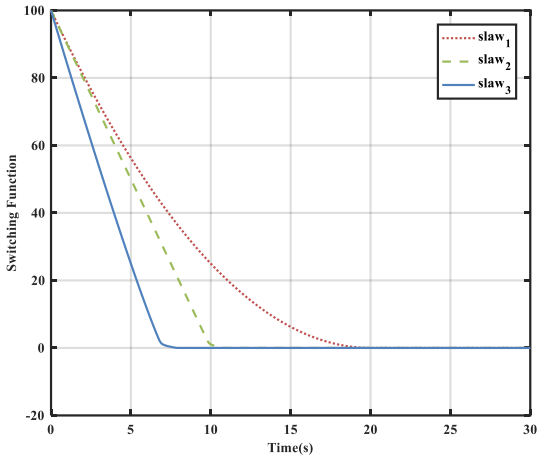

Fig.4 Switching function with different exponential reaching law

The result shows that improved exponential reaching law slaw_3 will not only increase reaching speed when switching function increase, but also avoid chattering when switching function is close to zero.

3.3. Analysis of quadratic integral sliding mode

It has been proved that SMC is insensitive to matched uncertainties[45]. But the robustness won't hold when it comes to mismatched uncertainties. Therefore, an auxiliary control u_1 is proposed based on quadratic integral sliding mode surface s_q to compensate impact caused by mismatched uncertainties.

Considering the uncertain system with mismatched uncertainties (9), the uncertainties are unknown, but it is acceptable to assume that the uncertainties are norm-bounded. Assumptions are introduced as follows:

Assumption 1 $\|\Delta f(x)\| \le \xi_1 \|x\| + \xi_0 \le \|f(x)\|$, with scalars $\xi_0 > 0$, $\xi_1 > 0$, here $\|\cdot\|$ stands for Euclidean norm and this definition remains unchanged in the remainder of this paper.

Assumption 2 $\|\Delta g(x)\| \le \zeta_1 \|x\| + \zeta_0 \le \|g(x)\|$, with scalars $\zeta_0 > 0$, $\zeta_1 > 0$

Assumption 3 $u_0 \le \beta_0 + \beta \|x\|$, with scalars $\beta_0 > 0$, $\beta_1 > 0$

Remark 5 The uncertainties are assumed to be norm-bounded and its upper bound is limited by a linear or nonlinear function, which is generally a sufficiently large function in form of $a\|x\| + b$. Though this assumption will bring conservativeness in study, it works in most real cases and be accepted in researches dealing with uncertainties[46,47].

In order to compensate the effect of mismatched uncertainties, s_q is designed as:

$$\begin{aligned} s_q = {} & \frac{1}{2}[x^T(t)x(t) - x(t_0)^T x(t_0)] \\ & - \int_{t_0}^{t} \{x^T(t)[f(x) + g(x)u] - b(x)u_1\} dt \end{aligned} \tag{13}$$

where $x(t_0)$ is the initial values of the state vector, $b(x) \in R$ is demonstrated in (14)

$$b(x)=\sigma+\zeta_0\|x\|+\zeta_1\|x\|^2+\left\|x^T(t)g(x)\right\| \quad (14)$$

with an arbitrary scalar $\sigma>0$.

Assuming that the quadratic integral sliding mode surface $s_q=0$ can be reached, it leads to

$$\frac{1}{2}[x^T(t)x(t)-x(t_0)^T x(t_0)] -\int_{t_0}^{t}\{x^T(t)[f(x)+g(x)u]-b(x)u_1\}dt=0 \quad (15)$$

and the following equation can be obtained

$$s_q=\int_{t_0}^{t}\{x^T(t)[\Delta f(x)+\Delta g(x)u]+b(x)u_1\}dt=0 \quad (16)$$

If the quadratic integral sliding mode surface (16) is reached and remains there, then

$$\dot{s}_q=x^T(t)[\Delta f(x)+\Delta g(x)u]+b(x)u_1=0 \quad (17)$$

The equivalent control of u_1 will be:

$$u_{1eq}=-\frac{x^T(t)[\Delta f(x)+\Delta g(x)u_0]}{[x^T(t)\Delta g(x)+b(x)]} \quad (18)$$

Substituting u_{1eq} into (9), then the system in sliding mode will be:

$$\dot{x}=f(x)+g(x)u_0+\Delta f(x)I_n\Gamma+\Delta g(x)u_0I_n\Gamma$$

where I_n is unit matrix, $\Gamma=1-\frac{x^T(t)[g(x)+\Delta g(x)]}{x^T\Delta g(x)+b(x)}$

It is evident that

$$\Gamma=\frac{b(x)-x^T(t)g(x)}{b(x)+x^T(t)\Delta g(x)} \quad (19)$$

Consider that

$$-\left\|x^T(t)g(x)\right\|\le -x^T(t)g(x)\le\left\|x^T(t)g(x)\right\|$$

$$-\zeta_1\|x\|^2-\zeta_0\|x\|\le x^T(t)\Delta g(x)\le\zeta_1\|x\|^2+\zeta_0\|x\|$$

Take **Assumption 2** and (18) into consideration, it would follow:

$$b(x)-x^T(t)g(x)\le\sigma+\zeta_1\|x\|^2+\zeta_0\|x\|$$

$$\sigma+\left\|x^T(t)g(x)\right\|\le x^T(t)\Delta g(x)+b(x)$$

then

$$\Gamma\le\frac{\sigma+\zeta_1\|x\|^2+\zeta_0\|x\|}{\sigma+\left\|x^T(t)g(x)\right\|}\le 1$$

Besides

$$0<\sigma\le b(x)-x^T(t)g(x)$$

$$0<\sigma\le b(x)-x^T(t)\Delta g(x)$$

One can obtain the conclusion:

$$0<\Gamma\le 1 \quad (20)$$

In researches about ISMC with projection matrix G [34], the $\Gamma\ge 1$. It is obviously that the result made in this paper is an improvement in robustness against mismatched uncertainties.

Remark 6: If the quadratic integral sliding mode surface is reached and remains there, the effect of uncertainties $\Delta f(x)+\Delta g(x)u_0$ can be compensated by u_1, achieving robustness to mismatched uncertainties. Besides, s_q is a class of integral sliding mode surface and system is on s_q from any initial state, therefore, the system is robust to mismatched uncertainties from any initial state.

3.4. Design of combined sliding mode control law

u_0 has been introduced above, and u_1 is the auxiliary control action that compensates the mismatched uncertainties, with definition as:

$$u_1=-b^{-1}(x)[(\lambda_0+\lambda_1\|x\|)s_q+(\eta_0+\eta_1\|x\|)\mathrm{sgn}(s_q)] \quad (21)$$

where $\lambda_0,\lambda_1,\eta_0,\eta_1\in R$ are scalars defined as follows:

$$\lambda_0\ge\frac{\varepsilon_1(\zeta_1\|x\|^2+\zeta_0\|x\|+\sigma)}{\sigma} \quad (22)$$

$$\lambda_1\ge 0 \quad (23)$$

$$\eta_0\ge\frac{\varepsilon_2(\zeta_1\|x\|^2+\zeta_0\|x\|+\sigma)}{\sigma} \quad (24)$$

$$\eta_1\ge(\sigma\delta)^{-1}[\xi_0+\zeta_0\beta_0+(\xi_1+\zeta_0\beta_1+\zeta_1\beta_0)\|x\|+\zeta_1\beta_1\|x\|^2] \quad (25)$$

The two approaching parameters ε_1 and ε_2 in (22),(24) are arbitrary positive scalars, δ is defined as $\delta=(\sigma+\zeta_0\|x\|+\zeta_1\|x\|^2)^{-1}$.

4. STABILITY OF CLOSED-LOOP SYSTEM

The reachability of combined sliding mode surface and the stability of closed-loop system under combined sliding mode control will be proved in this section.

4.1. Reachability of combined sliding mode surface

Proof: Because of improved exponential reaching law (12), it is obviously that $s_l\dot{s}_l<0$. Consequently, the linear sliding mode surface s_l is reachable.

Derivative s_q along time, and substitute systems (9) into (15), it would be followed

$$\dot{s}_q=x^T(t)[\Delta f(x)+\Delta g(x)u]+b(x)u_1$$

By the quadratic integral sliding mode control law (20)-(24), one can obtain

$$\begin{aligned}s_q\dot{s}_q&=x^T(t)\Delta f(x)s_q+s_qx^T(t)\Delta g(x)u\\&\quad+s_qb(x)\{-b^{-1}(x)[(\lambda_0+\lambda_1\|x\|)s_q+(\eta_0+\eta_1\|x\|)\mathrm{sgn}(s_q)]\}\\&=x^T(t)\Delta f(x)s_q+s_qx^T(t)\Delta g(x)u\\&\quad-(\lambda_0+\lambda_1\|x\|)s_q^{\,2}-(\eta_0+\eta_1\|x\|)|s_q|\end{aligned}$$

and

$$\begin{aligned}&s_qx^T(t)\Delta g(x)u\\&=s_qx^T(t)\Delta g(x)\left\{u_0-b^{-1}(x)\begin{bmatrix}(\lambda_0+\lambda_1\|x\|)s_q\\+(\eta_0+\eta_1\|x\|)\mathrm{sgn}(s_q)\end{bmatrix}\right\}\\&=s_qx^T(t)\Delta g(x)u_0\\&\quad-x^T(t)\Delta g(x)b^{-1}(x)\begin{pmatrix}(\lambda_0+\lambda_1\|x\|)s_q^{\,2}\\+(\eta_0+\eta_1\|x\|)|s_q|\end{pmatrix}\end{aligned}$$

and then

$$
\begin{aligned}
s_q\dot{s}_q &= x^T(t)\Delta f(x)s_q + s_q x^T(t)\Delta g(x)u_0 \\
&\quad -x^T(t)\Delta g(x)b^{-1}(x)\begin{pmatrix}(\lambda_0+\lambda_1\|x\|)s_q{}^2\\ +(\eta_0+\eta_1\|x\|)|s_q|\end{pmatrix} \\
&\quad -\left((\lambda_0+\lambda_1\|x\|)s_q{}^2+(\eta_0+\eta_1\|x\|)|s_q|\right) \\
&= x^T(t)\Delta f(x)s_q + s_q x^T(t)\Delta g(x)u_0 \\
&\quad -\left(1+x^T(t)\Delta g(x)b^{-1}(x)\right)\begin{bmatrix}(\lambda_0+\lambda_1\|x\|)s_q{}^2\\ +(\eta_0+\eta_1\|x\|)|s_q|\end{bmatrix}
\end{aligned}
$$

Because of **Assumption 1**, **Assumption 2** and **Assumption 3**, the expression above will be:

$$
\begin{aligned}
s_q\dot{s}_q &\le \left[(\xi_1\|x\|+\xi_0)+(\zeta_1\|x\|+\zeta_0)(\beta_0+\beta_1\|x\|)\right]\|x\||s_q| \\
&\quad +\left[x^T(t)\Delta g(x)b^{-1}(x)\right]\begin{bmatrix}(\lambda_0+\lambda_1\|x\|)s_q{}^2\\ +(\eta_0+\eta_1\|x\|)|s_q|\end{bmatrix} \\
&\quad -\left[(\lambda_0+\lambda_1\|x\|)s_q{}^2+(\eta_0+\eta_1\|x\|)|s_q|\right] \\
&\le \left[(\xi_1\|x\|+\xi_0)+(\zeta_1\|x\|+\zeta_0)(\beta_0+\beta_1\|x\|)\right]\|x\||s_q| \\
&\quad +\left[\|x\|(\zeta_1\|x\|+\zeta_0)b^{-1}(x)-1\right]\begin{bmatrix}(\lambda_0+\lambda_1\|x\|)s_q{}^2\\ +(\eta_0+\eta_1\|x\|)|s_q|\end{bmatrix}
\end{aligned}
$$

It would lead to

$$
\begin{aligned}
s_q\dot{s}_q &\le \left\{\xi_0+\zeta_0\beta_0+(\xi_1+\zeta_0\beta_1+\zeta_1\beta_0)\|x\|+\zeta_1\beta_1\|x\|^2\right\}\|x\|\cdot|s_q| \\
&\quad -\frac{\sigma+\left\|x^T(t)g(x)\right\|}{b(x)}(\lambda_0+\lambda_1\|x\|)s_q{}^2 \\
&\quad -\frac{\sigma+\left\|x^T(t)g(x)\right\|}{b(x)}(\eta_0+\eta_1\|x\|)|s_q|
\end{aligned}
$$

Consider equation (22) to (25), then

$$s_q\dot{s}_q \le -\varepsilon_1 s_q{}^2-\varepsilon_2|s_q|$$

In consequence, the quadratic integral sliding mode surface s_q can be reached in finite time and remains there.

This is the end of the proof.■

4.2. Stability of the closed-loop system in sliding mode

Proof:

Take **Remark 5** into consideration, assuming that C_l is properly chosen to place poles of closed-loop system in left half of S-plane[48]. Supposing that $f(x)=Ax$, where A is the system matrix, then eigenvalues value of $\left[I-\left[C_l g(x,t)\right]^{-1}C_l\right]A$ are negative definite. Therefore, $\left[I-\left[C_l g(x,t)\right]^{-1}C_l\right]A$ is a negative definite matrix.

Select the Lyapunov function as

$$V(x)=\frac{1}{2}x^T(t)x(t) \tag{26}$$

$$
\begin{aligned}
\dot{V}(x) &= x^T(t)\dot{x}(t) \\
&= x^T(t)\begin{bmatrix}f(x)+\Delta f(x)\\ +g(x)u+\Delta g(x)u\end{bmatrix}
\end{aligned} \tag{27}
$$

The quadratic integral sliding mode surface (14) has been proved to be reachable. If the system reach the surface and remains there, then

$$x^T(t)[\Delta f(x)+\Delta g(x)u]-b(x)u_1=0 \tag{28}$$

Substitute equation (28) into equation (27), one can obtain

$$\dot{V}(x)=x^T(t)[f(x)+g(x)u_0-b(x)u_1] \tag{29}$$

When (15) is reached, then $u_1=0$ and equation (29) will be

$$
\begin{aligned}
\dot{V}(x) &= x^T(t)[f(x)+g(x)u_0] \\
&= x^T(t)\left[I-\left[C_l g(x)\right]^{-1}C_l\right]Ax(t)
\end{aligned} \tag{30}
$$

Because of the fact that $\left[I-\left[C_l g(x,t)\right]^{-1}C_l\right]A$ is a negative definite matrix, the quadratic form of $\left[I-\left[C_l g(x,t)\right]^{-1}C_l\right]A$ is negative definite, in other words, $\dot{V}(x)<0$.

Consequently, a positive definite Lyapunov function will give negative definite derivative with respect to time along the state, and the closed-loop system is asymptotically stable.

It can be seen that, if u_0 is designed to stabilized the nominal system (10), the closed-loop system with mismatched system (9) is asymptotically stable under the combined sliding mode control law u.

This is the end of proof.■

Remark 7: The design of u_0 and u_1 is proved to be separate. This study is focused on combining SMC (u_0) with an auxiliary control u_1 based on s_q to achieve robustness to mismatched uncertainties. Moreover, various control method including LQR, H-infinity can be applied in u_0 designing to achieve additional advantages, on the condition that u_0 can stablize nominal system (10). Applying other method in u_0 designing deserves our investigations in future works.

Remark 8: No matter what method are adopted in u_0 designing, auxiliary control u_1 will enhance its robustness to mismatched uncertainties, results in an advantages that the design of u_0 and u_1 are separate. Therefore, u_0 is simplely aimed at nominal system, bring much convenience in real practice.

Remark 9: The computational load of CSMC is heavier than SMC, due to a sliding mode surface in quadratic form. In simulation test, CSMC's single step costs 0.0013s~0.0020s, while SMC's single step costs 0.0005s~0.0009s. But the computational limitation could be lessened along with improvement in micro control chips.

5. SIMULATION

The combined sliding mode control could be applied to the uncertain system with linear time-invariant nominal plants, where $f(x,t)=Ax$, $g(x,t)=B$, A is the system matrix and B is the input matrix.

The parameters of a electric fuel pump are used in simulation test, which are is shown in the following table.

Table1. Parameters of EFP in MEEs

Parameter	Unit	Value
ε		1.37
R_1	mm	16.5
R_e	mm	19.5
h	mm	1
ρ	kg/m^3	960
μ	$Pa \cdot s$	0.048
K_e	V / rad	0.0482
B	mm	10
Δp	MPa	1
R	Ω	0.488
L	mH	1.19
J_1	$Kg \cdot m^2$	1.89×10^{-6}
J_2	$Kg \cdot m^2$	0.362×10^{-3}

Substitute parameters into system (9), it would be:

$$\begin{bmatrix}\dot{x}_1\\ \dot{x}_2\\ \dot{x}_3\\ \dot{x}_4\\ \dot{x}_5\end{bmatrix}=\begin{bmatrix}x_3\\ x_4\\ -43.5489x_1+43.5489x_2-0.0435x_3+0.0435x_4+132.4374x_5-15.27\\ 43.7762x_1-43.7762x_2+0.0438x_3-0.0438x_4-15.27\\ -40.5020x_3-410.08x_5+420.1681u\end{bmatrix},$$

$$+\Delta f(x,t)+\Delta g(x,t)u$$

$C_l=\begin{bmatrix}-15.0978 & 15.0978 & 35.2190 & 2.3231 & 364.1673\end{bmatrix}$

, $\text{slaw}=-1\times\left[0.1+(1-0.1)e^{-|s_l|^2}\right]^{-1}|s_l|^{0.1}\text{sgn}(s_l)$,

$D=0.1216$, $u_0=(420.1681)^{-1}(C_l x+\text{slaw})$.

Set the initial state to be $x_0=[0\quad 0\quad 1\quad 0\quad 0]^T$, with $\sigma=1$, $\zeta_0=1$, $\zeta_1=1$, $\lambda_0=60$, $\lambda_1=0$, $\eta_0=1$, $\eta_1=4$. Parameters are chosen according to (22)-(25) to gurantee the stability of closed-loop system. Parameters perturbations are generally fluctuate around the regular point, and $\Delta f(x)=10\%f(x)$, $\Delta g(x)=-10\%g(x)$ are used to reflect its effects on system state and degeneration in control channel.

External disturbances are divided into 3 type: Time-invariant matched d_1, Time-invariant mismatched d_2, Time-variant mismatched d_3. External disturbances will act on system to verify its robustness.

The red line stands for SMC (u_0) and blue line stands for CSMC(u_0+u_1).

When there is matched uncertainties $d_1=[0\quad 0\quad 0\quad 0\quad 5]^T$ acting on system at 2 seconds, the system's response is shown in Fig.3 and Fig.4 .

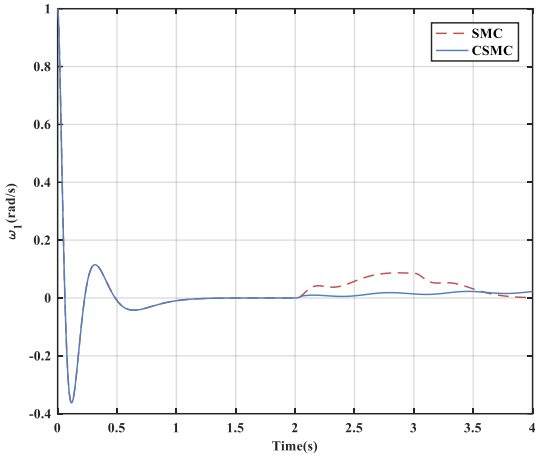

Fig.3 Angular velocity of driving gear with d_1

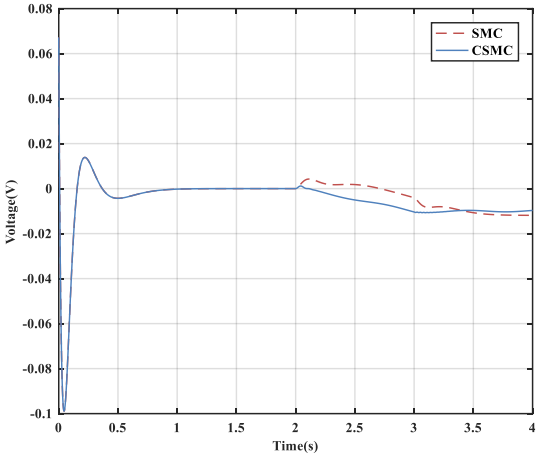

Fig.4 Control voltage with d_1

Before 2 seconds, it is obviously that SMC has same responses as CSMC, because there is no uncertainties and $u_1=0$, $u=u_0$. Responses change when there are uncertainties and $u_1\neq 0$, $u=u_1+u_0$. According to Fig.3, the effects of uncertainties are compensated by u_1, enhancing system's robustness.

When mismatched time invariant uncertainties $d_2=[0\quad 0\quad 1\quad 1\quad 0]^T$ acting on system at 2 seconds, the simulation result is presented in Fig.5 and Fig.6.

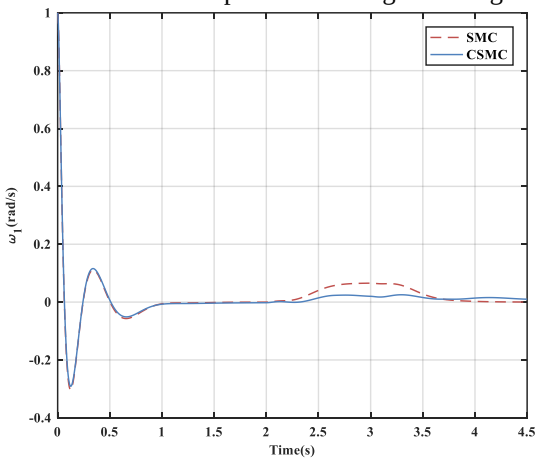

Fig.5 Angular velocity of driving gear with d_2

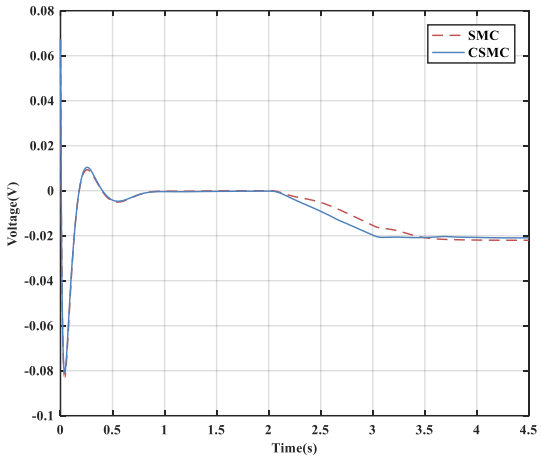

Fig.6 Control voltage with d_2

Fig.5 and Fig.6 illustrate that CSMC has slightly fluctuation when system is affected by mismatched uncertainties. As a contrary, SMC has comparatively fierce fluctuation, which costs 1.7s to be compensated. The results verify that CSMC has better robustness against mismatched uncertainties than SMC, and u_1 force uncertainties slide along s_q , compensating its influences.

When time variant mismatched uncertainties $d_3 = [0 \quad 0 \quad 1.5\sin t \quad 1.5\sin t \quad 0]^T$ is added into system at 2 seconds, the results are shown as follows：

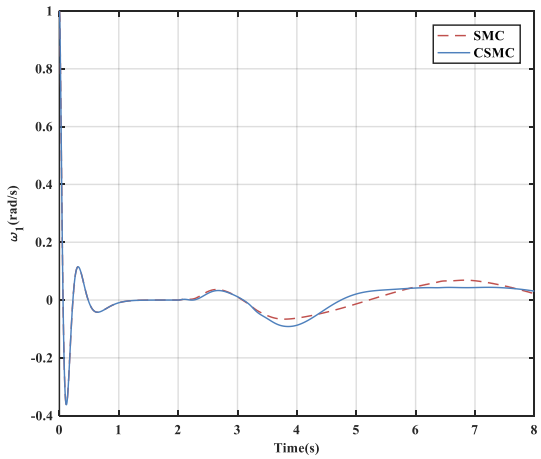

Fig.7 Angular velocity of driving gear with d_3

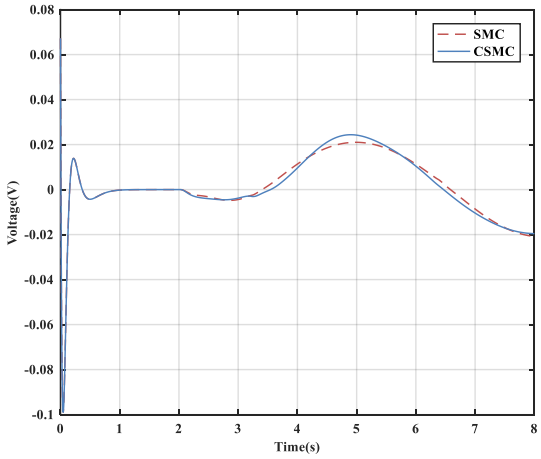

Fig.8 Control voltage with d_3

As shown in Fig.7 and Fig.8, the fluctuation of CSMC is comparatively smooth and steady in comparison with SMC. CSMC still remain robust when mismatched uncertainties are time variant, as long as they are norm-bounded.

The simulation results verify the effectiveness of CSMC in enhancing robustness and reducing chattering.

6. CONCLUSION

Aimed at EFP system, a class of uncertain system with matched and mismatched uncertainties is studied. A novel robust control method CSMC is proposed to enhance SMC's robustness to mismatched uncertainties. The main results of this paper are as follows:

(1) Mathematical model of electric fuel pump system equipped in MEEs is established based on dynamic analysis, in which, leakages and variant load are taken into consideration. When compared to models based on local linearization, model in this paper is more practical with wider working range, promoting concerned researches especially in control area.

(2) A novel robust control method based on combined sliding mode surface is proposed. u_0 is based on linear sliding mode surface with improved exponential reaching law , to stablize nominal system. And auxiliary control u_1 based on quadratic integral sliding mode surface is used to compensate the influence caused by mismatched uncertainties, enhancing system's robustness.

(3) Improved exponential reaching law is applied in CSMC, to achieve adaptive convergence rate. The convergence rate will not only increase reaching speed when switching function increase, but also avoid chattering when switching function is close to zero.

(4) It is theoretially proved that CSMC has robustness to mismatched uncertainties. And results of CSMC has less conservativeness than present results.

(5) The comprehensive proof of reachability of CSMC and stability of closed-loop system is given. In addition, a detailed analysis of system in sliding mode is shown as well.

(6) Simulations are carried out in comparison with SMC, verifying the effectiveness of proposed method.

(7) The computational burder of CSMC is 2-3 times heavier that that of SMC, which is a challenge in practicing CSMC.

(8) u_0 and u_1 can be designed separately. u_1 has no effect on u_0 . This feature bring much convinence in practice. Applying other method in u_0 designing deserves investigations in future works. Additionally, arbitrary existing system (stabilized by u_0) satisfying **Assumption 1-3** can be expanded with u_1 to enhance its robustness (The expanded system is controlled by $u_0 + u_1$).

APPENDIX

Notation

θ_1 Angular displacement of the driving gear

θ_2 Angular displacement of the driven gear

ω_1 Angular velocity of the driving gear

ω_2 Angular velocity of the driven gear
J_1 Moment of inertia of the driving gear
J_2 Moment of inertia of the driven gear
R_e Radius of addendum
R_1 Circle radius of driving gear
R_2 Circle radius of driven gear
B Tooth thickness
Δp Pressure difference
M_1 Equivalent torque on driving gear
M_2 Equivalent torque on driven gear
k_1 Equivalent damping coefficient
k_2 Equivalent stiffness coefficient
K_e Back-EMF coefficient
i_a Current in BLDC motor in one phase,
u_a , u_b Stator voltages
L Equivalent common reactance
q_v Instantaneous flow of gear pump
h_1 Addendum height of the driving gear
h_2 Addendum height of the driven gear
f The distance between the engaging point and the pitch point
Q_v Theoretical flow of gear pump
t_0 The base pitch of gear
f_0 The length of actual meshing line
Q_l Seal face leakage
Q_s The radial leakage
R_f Radius of dedendum circle
R_z Radius of gear shafts
Q_r Real flow of gear pump
μ Coefficient of kinetic viscosity of the working medium
S Tooth thichness.

Abbreviations

AGB—Accessory Gear Box
MEE—More-electric Engine
EMA—Electro-Mechanical Actuator
MEA—More-electric Aircraft
BLDC motor—Brushless Direct Current motor
ACOC—Air-Cooled Oil Cooler
SFC—Specific Fuel Consumption
FADEC—Full Authority Digital Electronic Control
FMU—Fuel Management Unit
SMC—Sliding Mode Control
ISMC—Integral Sliding Mode Control
FISMC—Fuzzy Integral Sliding Mode Control
CSMC—Combined Sliding Mode Control

REFERENCES

[1] Steimes, J. and P. Hendrick, "Dimensional analysis of an integrated pump and de-aerator solution in more electric aero engine oil systems," *Aeronautical Journal -New Series-*, 121.1240(2017):1-18.

[2] Provost, M. J, "The More Electric Aero-engine: a general overview from an engine manufacture," *Power Electronics, Machines and Drives, 2002. International Conference on* IET, 2002:246-251.

[3] Hirst, M., et al. "Demonstrating the more electric engine: a step towards the power optimised aircraft," *IET Electric Power Applications*, 5.1(2011):3-13.

[4] Oyori, Hitoshi, N. Morioka, and T. Fukuda. "Conceptual Study of Low-Pressure Spool-Generating Architecture for More Electric Aircraft," *SAE 2015 AeroTech Congress & Exhibition*, 2015.

[5] Morioka, Noriko, and H. Oyori. "Fuel Pump System Configuration for the More Electric Engine," *Aerospace Technology Conference and Exposition*, 2011.

[6] Pickert, Volker, et al. "Forced Commutated Controlled Series Capacitor Rectifier for More Electric Aircraft," *IEEE Transactions on Power Electronics*, PP.99(2018):1-1..

[7] Peng, Kai, et al. "Development and test evaluation of full authority digital electronic control system for auxiliary power unit based on electronic pump," *IEEE International Conference on Signal Processing, Communications and Computing*, 2016:1-4.

[8] Morioka, N., and H. Oyori. "More electric architecture for engine and aircraft fuel system," *SAE Technical Papers*, 8(2013).

[9] Morioka, Noriko, et al. "Development of the Electric Fuel System for the More Electric Engine," *ASME Turbo Expo 2014: Turbine Technical Conference and Exposition American Society of Mechanical Engineers*, 2014:V006T06A018-V006T06A018.

[10] Amrhein, Marco, et al. "Integrated Electrical System Model of a More Electric Aircraft Architecture," *SAE 2008 Power Systems Conference*, 2008.

[11] Ferreira, André Morais, et al. "Development of 1D Simulation Model of Electric Fuel Pump for Flex-Fuel Application," *SAE Brasil International Congress and Display*, 2016.

[12] Motapon, Souleman Njoya, L. A. Dessaint, and K. Al-Haddad. "A Comparative Study of Energy Management Schemes for a Fuel-Cell Hybrid Emergency Power System of More-Electric Aircraft," *IEEE Transactions on Industrial Electronics* 61.3(2013):1320-1334.

[13] Mecrow, B. C., et al. "Design and testing of a four-phase fault-tolerant permanent-magnet machine for an engine fuel pump," *IEEE Transactions on* Energy Conversion 19.4(2004):671-678.

[14] Wang, Li Guo, et al. "Application of Variable PID Law in Electric Gear Fuel Pump," *Journal of Astronautic Metrology & Measurement* (2015).

[15] Chen, Zhong, Z. D. Zhang, and W. U. Shuai. "Numerical simulation of the internal flow and structural improvement in the electrical fuel pump," *Journal of Mechanical & Electrical Engineering* (2016).

[16] Utkin, Vadim I., and H. C. Chang. “Sliding mode control on electro-mechanical systems,” *Mathematical Problems in Engineering* 8.4-5(2002):451-473.

[17] Shtessel Y B, Moreno J A, Fridman L M. “Twisting sliding mode control with adaptation: Lyapunov design, methodology and application,” *Automatica*, 2017, 75:229-235.

[18] Han Y, Kao Y, Gao C. “Robust sliding mode control for uncertain discrete singular systems with time-varying delays and external disturbances,” *Automatica*, 2017, 75(4):210-216.

[19] Sun, Haibin, et al. “Fixed-time attitude tracking control for spacecraft with input quantization,” *IEEE Transactions on Aerospace & Electronic Systems* PP.99:1-1.

[20] Ginoya, Divyesh, P. D. Shendge, and S. B. Phadke. “Sliding Mode Control for Mismatched Uncertain Systems Using an Extended Disturbance Observer,” *IEEE Transactions on Industrial Electronics* 61.4(2013):1983-1992.

[21] Monteiro, J. R. B. A., C. M. R. Oliveira, and M. L. Aguiar. “Sliding mode control of brushless DC motor speed with chattering reduction,” *IEEE, International Symposium on Industrial Electronics*, 2015:542-547.

[22] Sunila M S, Sankaranarayanan V, Sundereswaran K. “Optimised sliding mode control for MIMO uncertain non-linear system with mismatched disturbances,” *Electronics Letters*, 2018, 54(5):290-291.

[23] Lu B, Fang Y, Sun N. “Continuous Sliding Mode Control Strategy for a Class of Nonlinear Underactuated Systems,” I*EEE Transactions on Automatic Control*, 2018, PP(99):1-1.

[24] Qi, Wenhai, G. Zong, and H. R. Karim. “Observer-Based Adaptive SMC for Nonlinear Uncertain Singular Semi-Markov Jump Systems With Applications to DC Motor.” *IEEE Transactions on Circuits & Systems I Regular Papers* PP.99(2018):1-10.

[25] Draenovi, B. “The invariance conditions in variable structure systems.” *Pergamon Press, Inc*. 1969.

[26] Tsai, Yao Wen, and V. A. Duong. “Necessary and sufficient invariance conditions in mismatched uncertain variable structure systems,” *Journal-Chinese Institute of Engineers*,40.5(2017):1-10.

[27] Wang, Yueying, et al. “Dissipativity-Based Fuzzy Integral Sliding Mode Control of Continuous-Time T-S Fuzzy Systems,” *IEEE Transactions on Fuzzy Systems*, 26.3(2018):1164-1176.

[28] Pan Y, Joo Y H, Yu H. “Discussions on Smooth Modifications of Integral Sliding Mode Control,” *International Journal of Control Automation & Systems*, 2018, 16(2):586-593.

[29] Wang, Yueying, et al. “Fuzzy-Model-Based Sliding Mode Control of Nonlinear Descriptor Systems,” *IEEE Transactions on Cybernetics*, PP.99:1-11.

[30] Song, et al. “Three-dimensional guidance law based on adaptive integral sliding mode control,” *Chinese Journal of Aeronautics*, 29.1(2016):202-214..

[31] Wang, Yueying, et al. “Sliding Mode Control of Fuzzy Singularly Perturbed Systems With Application to Electric Circuit,” *IEEE Transactions on Systems Man & Cybernetics Systems*, PP.99(2017):1-9.

[32] Zhang, Jinhui, et al. “Disturbance Observer-Based Integral Sliding-Mode Control for Systems With Mismatched Disturbances,” *IEEE Transactions on Industrial Electronics* 63.11(2016):7040-7048.

[33] Mnasri, Chaouki, D. Chorfi, and M. Gasmi. “Robust Integral Sliding Mode Control of Uncertain Networked Control Systems with Multiple Data Packet Losses,” *International Journal of Control Automation & Systems*(2018):1-10.

[34] Castanos, F., and L. Fridman. “Analysis and design of integral sliding manifolds for systems with unmatched perturbations,” *IEEE Transactions on Automatic Control* 51.5(2006):853-858.

[35] Li, Yulong, and F. Sun. “Theoretical analysis of volumetric efficiency and phenomenon of trapped oil under centrifugation in external spur-gear pump,” *Transactions of the Chinese Society of Agricultural Engineering*, 27.3(2011):147-151.

[36] Li, Yulong, and K. Liu. “Dynamic Model of Trapped Oil and Effect of Related Variables on Trapped Oil Pressure in External Spur-gear Pump,” *Transactions of the Chinese Society for Agricultural Machinery*, 40.9(2009):214-219.

[37] Jia, Hong Ping, and H. F. Wei. “Variable Structure Sliding Mode Current Control of BLDCM,” *Micromotors* (2010).

[38] Kong, Fanyu, et al. “Analysis of influence factors on flow rate characteristics in gear pump,” *Journal of Drainage & Irrigation Machinery Engineering*, 32.2(2014):108-112.

[39] Zhang, Yong Xiang, and J. Jin. “Analysis of Instantaneous Flow and Restraint of Pulsation for External Gear Pump,” *Chinese Hydraulics & Pneumatics* (2015).

[40] Zhao, Dexin, R. Yuan, and J. Luo. “The Research On Pure Water Hydraulic External Gear Pump,” *Applied Mechanics & Materials*, 44-47(2011):1767-1772.

[41] Jun, M. A. “Analysis and Calculation of Outer-engaged Gear Pump's Leakage,” *Coal Mine Machinery* (2011).

[42] Trivedi, P. K., and B. Bandyopadhyay. “Non unique equivalent control in sliding mode with linear surfaces,” *International Conference on Power, Control and Embedded Systems* IEEE, 2010:1-5.

[43] Fallaha, Charles J., et al. “Sliding-Mode Robot Control With Exponential Reaching Law,” *IEEE Transactions on Industrial Electronics* 58.2(2011):600-610.

[44] Devika, K. B, and S. Thomas. “Power rate exponential reaching law for enhanced performance of sliding mode control,” *International Journal of Control Automation & Systems* 15.6(2017):2636-2645.

[45] Castaños, Fernando, J. X. Xu, and L. Fridman. “Integral Sliding Modes for Systems with Matched and Unmatched Uncertainties,” (2006).

[46] Park, P. G., D. J. Choi, and S. G. Kong. “Output

feedback variable structure control for linear systems with uncertainties and disturbances ☆," *Automatica* 43.1(2007):72-79.

[47] Han, Ho Choi. "Variable structure output feedback control design for a class of uncertain dynamic systems ☆," *Automatica* 38.2(2002):335-341.

[48] Wei, W. U. "Multi-UAV Autonomous Formation Attitude Control Based on Eigenvalue Placement Sliding Mode Control," *Measurement & Control Technology* (2015).

Lingfei Xiao currently holds the position of Associate Professor within the Jiangsu Province Key Laboratory of Aerospace Power Systems, College of Energy and Power Engineering, Nanjing University of Aeronautics and Astronautics. She received Ph.D. degree from Zhejiang University in 2008 and as a Visitor Scholar in the Department of Automatic Control and Systems Engineering, the University of Sheffield, UK, in 2013. Her main research interest lies in the advanced control theory and application in complex mechanical and electrical systems, and aircraft engine systems.

Runze Ding born in 1993, is currently a master candidate at Nanjing University of Aeronautics and Astronautics. His research interest is aircraft engine control systems.

Appendices